Hindawi Publishing Corporation
EURASIP Journal on Wireless Communications and Networking
Volume 2008, Article ID 352597, 10 pages
doi:10.1155/2008/352597

Research Article

Turbo Decision Aided Receivers for Clipping Noise Mitigation in Coded OFDM

Maxime Colas,[1] Guillaume Gelle,[1] and David Declercq[2]

[1] *Décom-Crestic Lab, University of Reims Champagne-Ardenne, BP 1039, 51687 Reims Cedex 2, France*
[2] *ETIS Lab, Ecole Nationale Supérieure de l'Electronique et de ses Applications, 6 Avenue du Ponceau, 95014 Cergy Pontoise Cedex, France*

Correspondence should be addressed to Guillaume Gelle, guillaume.gelle@univ-reims.fr

Received 11 July 2006; Revised 26 January 2007; Accepted 31 August 2007

Recommended by Luc Vandendorpe

Orthogonal frequency division multiplexing (OFDM) is the modulation technique used in most of the high-rate communication standards. However, OFDM signals exhibit high peak average to power ratio (PAPR) that makes them particularly sensitive to nonlinear distortions caused by high-power amplifiers. Hence, the amplifier needs to operate at large output backoff, thereby decreasing the average efficiency of the transmitter. One way to reduce PAPR consists in clipping the amplitude of the OFDM signal introducing an additional noise that degrades the overall system performance. In that case, the receiver needs to set up an algorithm that compensates this clipping noise. In this paper, we propose three new iterative receivers with growing complexity and performance that operate at severe clipping: the first and simplest receiver uses a Viterbi algorithm as channel decoder whereas the other two implement a *soft-input soft-output* (SISO) decoder. Each soft receiver is analyzed through EXIT charts for different mappings. Finally, the performances of the receivers are simulated on both short time-varying channel and AWGN channel.

1. INTRODUCTION

Orthogonal frequency division multiplexing (OFDM) is a modulation technique used in many new and emerging broadband technologies either wired for the ADSL (asymmetric digital subscriber line) or wireless single or multiusers as in DAB (digital audio broadcasting), DVB-T (digital video broadcasting-terrestrial), wireless LANs, and so forth [1]. In all these systems, the information data stream is transmitted in parallel on several orthogonal subcarriers, each subcarrier being QAM or PSK modulated. The main advantage of OFDM is both its bandwidth efficiency and its ability to counter multipath fading without requiring complex equalizer [2]. Moreover, OFDM can be easily implemented using FFT. However, a well-known drawback of OFDM is that transmitted signals exhibit a Gaussian time-domain waveform with large amplitude range and high peak to average power ratio (PAPR) which make OFDM particularly sensitive to nonlinear distortions caused by the high power amplifier (HPA). Classically, the mitigation of these nonlinear distortions is partially performed by a pre-distorter which inverts the HPA characteristic [3, 4]. Additionally, the HPA operates at a large power input backoff (IBO) to ensure a distortionless transmission. So, the obvious disadvantage of fixing a large IBO is that the maximum transmission power is much higher than necessary.

Two kinds of approaches can be distinguished to deal with high PAPR signals. The first approach is to generate OFDM signals with a low PAPR without information loss. Many of these PAPR reduction techniques have been proposed in the literature, using selective mapping [5, 6] or phase shifting [7]. The second way to reduce the PAPR is deliberately to clip the peaks with high amplitude [8]. The power ratio in dB between the squared clipping amplitude A^2 and the OFDM signal power σ_x^2 is called clipping ratio (CR). Clearly, the clipping operation causes some degradation due to the nonlinear operation which requires specific compensation. Two classes of clipping techniques have been described in the literature as follows.

(1) The first one clips the OFDM signal after oversampling of the output of the IFFT. The clipping operation causes both in-band and out-of-band (OOB)

distorsion of the OFDM signal. The OOB distorsion can be mitigated by bandpass filtering which in turn causes some peak regrowth [9].

(2) The second approach proposes to clip the OFDM samples without interpolation. In that case, the bandpass filtering for OOB radiation removal is useless because all the clipping noise falls in band. Hence, this operation must be associated with efficient in-band noise mitigation receivers [10, 11].

In this paper, we focus on the latter clipping technique, which requires clipping noise mitigation at the Nyquist sampling rate only. Assuming that the HPA-IBO is fixed at a sufficiently high level, the power amplifier operates in its linear region and thus only the problem of in-band noise mitigation is considered. However, the algorithms presented can readily be extended for oversampled OFDM frames.

When using deliberate clipping, the receiver needs to rebuild the clipped peaks before the symbol detection in order to compensate the information loss. An attractive method has been proposed in [10, 11], which consists in the iterative reconstruction of the peak amplitudes by successive hard decisions both in time and frequency domain. This method is called decision-aided reconstruction (DAR). When using coded OFDM modulation as in wireless communication systems on severe fading mutipath channels, it can be interesting to jointly use the channel decoder and the clipping noise mitigation process (DAR). The purpose of this paper is to provide some insights on the joint decoding/clipping noise mitigation through the introduction of a class of algorithms named Turbo-DAR (*turbo decision-aided reconstruction*) which are able to operate at severe clipping ratios. The guiding principle of a Turbo-DAR receiver is to perform several iterations of a receiver composed of a clipping noise mitigation block and a channel decoder, in a turbo fashion.

We present three Turbo-DAR receivers for convolutionally coded transmission, with growing complexity and performance. The simplest receiver uses a Viterbi decoder, and is therefore called Hard-Turbo-DAR. The second receiver uses a soft-input soft-output (SISO) decoder (BCJR algorithm) in place of the Viterbi decoder and is called Soft-Turbo-DAR. Finally, we take advantage of the bit interleaved coded modulation (BICM) structure of the receiver and propagates the soft extrinsic information backward to the symbol demapper. This receiver is called Turbo-DAR-BICM.

An approach similar to the Soft-Turbo-DAR has already been proposed in [12], however, our system mitigates the clipping noise whereas their receiver iteratively estimates and substracts the Bussgang noise from oversampled OFDM signals, which is less general.

Thanks to the propagation of soft extrinsic values, the Soft-Turbo-DAR and the Turbo-DAR-BICM can be theoretically studied with the help of well-known EXIT charts [13]. We have therewith compared the different receiver behaviors with respect to the symbol mapping of the QAM constellation, and we especially show that the mapping has to be chosen carefully for each receiver type.

The paper is organized as follows. In Section 2, we make a brief presentation of the communication system and the introduction of useful notations. Then, the three receivers (Hard-Turbo-DAR, Soft-Turbo-DAR and Turbo-DAR-BICM) are presented in detail in Section 3. A convergence analysis with EXIT charts is presented in Section 4 for the two latter receivers, and a discussion about the suited mapping choice is given. Finally, in Section 5, we discuss the validity of our approach and the advantages of our receivers based on simulations over AWGN and slow time-varying frequency selective (STVFS) channels. We show in particular that the Turbo-DAR receivers can compensate for almost all the clipping noise for CR as small as 1 dB. This result is really interesting since it shows that one can possibly accept a much lower CR than those usually used in practice, thereby improving the power efficiency of the OFDM transmission.

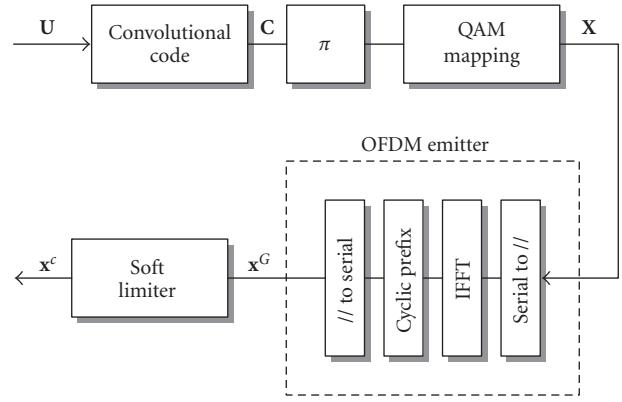

Figure 1: OFDM transmission system with soft limiter that simulates the power amplifier effect.

2. TRANSMITTER AND CHANNEL MODEL

In the sequel, capital letters stand for frequency domain signals and bold notations represent frame vectors. The $\cdot^{\dagger}$ operator denotes an interleaved vector or the interleaved values of a vector. As described on Figure 1, a length K_b binary sequence $\mathbf{U}$ is encoded via a convolutional code to obtain a length N_b coded binary sequence $\mathbf{C}$. Then, the sequence $\mathbf{C}$ is interleaved with a pseudorandom interleaver $\{\pi(n)\}_{n=0..N_b-1}$, and we denote by $\mathbf{C}^{\dagger}$ the output of the interleaver. $\mathbf{C}^{\dagger}$ is mapped on $N_b/\log_2(M) = N$ symbols $\mathbf{X}$ belonging to a M-QAM constellation. The output of the OFDM modulator is obtained with an N-point inverse fast Fourier transform (IFFT) as

$$x_n = \frac{1}{\sqrt{N}} \sum_{k=0}^{N-1} X_k \exp \frac{2j\pi nk}{N}, \quad 0 \le n \le N-1, \tag{1}$$

where $\mathbf{X} = \{X_k\}_{k=0}^{N-1}$ are the coded QAM symbols and N is the OFDM block size.

In order to cancel both the inter carrier and inter-block interference, a cyclic prefix is added to the OFDM block as

$$x_n^G = x_{(n+N-G)_N}, \quad 0 \le n \le N+G-1, \tag{2}$$

where G the length of the cyclic prefix is assumed to be longer than the channel memory, and $(k)_N$ is the residue of

k modulo N. Finally, the clipping operation is implemented with a soft limiter applied on the time-sequence $\mathbf{x}^G$ as follows:

$$x_n^c = \begin{cases} x_n^G & |x_n^G| \le A,\ 0 \le n \le N+G-1, \\ A\exp\left(\arg x_n^G\right) & |x_n^G| > A,\ 0 \le n \le N+G-1, \end{cases} \tag{3}$$

where $\mathbf{x}^c = \{x_n^c\}_{n=0}^{N+G-1}$ is the clipped output sequence and A is the clipping amplitude. This clipping operation applies only on the amplitude of the OFDM values, and the phase of the OFDM values remain unchanged.

The clipping ratio (CR) is defined as

$$\mathrm{CR} = 10\log_{10}\frac{A^2}{\sigma_x^2}\ \mathrm{dB}, \tag{4}$$

where σ_x^2 is the mean power of the OFDM symbols before clipping.

The samples $\mathbf{x}^c$ are then transmitted through a channel defined by its spectrum $\{H_k\}_{k=0..N-1}$. In this paper, two types of channels are considered: the AWGN channel with M-QAM inputs for which the spectrum is flat $H_k = C^{te}$, and a frequency selective channel which could vary from one OFDM block to another, that we call *slow time-varying frequency selective* (STVFS) channel. Although the channel could vary, we assume that an accurate estimator of the channel spectrum is available at the receiver. We also assume a perfect carrier and timing synchronization of the receiver. Moreover, considering the clipped signal sampled at the Nyquist rate and a linear power amplification, the impact of the OOB radiation will not be addressed in the paper. So only the in-band noise is mitigated by our algorithms.

Throughout this paper, we define E_b/N_0 as the mean transmitted energy per information bit to channel noise power ratio

$$\frac{E_b}{N_0} = \frac{E_s E_{\mathrm{ch}}(N+G)}{2R\cdot\sigma_b^2\cdot\log_2(M)N}, \tag{5}$$

where R is the coding rate of the convolutional code, σ_b^2 is the variance on the real and imaginary parts of the channel noise, $E_{\mathrm{ch}} = \sum_k |H_k|^2$ represents the channel gain, and G/N is the additional energy ratio required for the transmission of the cyclic prefix. The mean power per symbol sent through the channel is denoted E_s. Assuming that the OFDM signal is composed of i.i.d. samples distributed as complex Gaussian, E_s depends on the clipping level A and on the constellation power P_c such as $E_s = P_c(1-\exp(-A^2/P_c))$. In the sequel, we use rectangular M-QAM constellation with symbols on odd integer coordinates, so $P_c = 2(M-1)/3$.

In the next section, we describe a class of iterative receivers with growing complexity, whose goal is to solve efficiently the estimation and reconstruction of the clipping noise.

3. CLASS OF TURBO-DAR RECEIVERS

3.1. General principle

According to Figure 2, the signal at the receiver input after cyclic prefix removal is transformed by a direct N-points FFT and equalized to compensate for the channel selectivity (only for the STVFS channel). The equalizer used in our study is the MMSE equalizer in the frequency domain, performed by multiplying each subcarrier of the OFDM block by

$$K_k = \frac{H_k^*}{|H_k|^2 + N_0/E_s}, \quad k = 0\cdots N-1. \tag{6}$$

The choice of the MMSE equalizer is motivated by the fact that it reduces the amplitude of the errors and prevents error propagation during the iterative process. We have compared the receiver performance with other types of equalizers to verify this statement.

The principle basis of Turbo-DAR receivers is to iterate between the *symbol decoder,* which is composed of an FEC decoder and a symbol mapper, and the decision-aided reconstruction (DAR) of the clipping noise only. In Figure 2, the symbol decoder corresponds to the Hard-Turbo-DAR that is presented in detail in the next section. Using this type of receiver, the FEC code aims at correcting the additive white Gaussian noise and a small part of the clipping noise, while the DAR loop is used to help the FEC decoder by correcting part of the clipping noise. All receivers described in this paper focus on improving the cooperation between these two blocks (symbol decoder and DAR loop).

The clipping amplitude defined in (3) is assumed to be known at the receiver side and is used in the DAR loop for the detection of peaky samples. One iteration of a Turbo-DAR receiver is described thereafter, and only the structure of the *symbol detector* changes from one Turbo-DAR receiver to another.

(1) The equalized signal $\mathbf{Z}$ serves as initialization at the first iteration $\widetilde{\mathbf{X}}^{(0)} = \mathbf{Z}$.

(2) In the ith ≥ 1 iteration, the noisy symbols $\widetilde{\mathbf{X}}^{(i)}$ feed the symbol decoder. The symbol decoder aims at denoising the QAM symbols with the help of the channel decoder. The three steps of the symbol decoder are then (i) a QAM demapper that is performed with the maximum a posteriori (MAP) criterion, (ii) a channel decoder that is either hard output or soft output, depending on the Turbo-DAR receiver type, and (iii) a symbol mapper that transforms the output of the channel decoder into symbols of the QAM constellation (hard output case), or soft symbols (soft output case). The output of the symbol decoder is denoted $\widehat{\mathbf{X}}^{(i)}$.

(3) The values $\widehat{\mathbf{X}}^{(i)}$ are propagated backwards to the input of the symbol decoder through the DAR loop. In the DAR loop, $\widehat{\mathbf{X}}^{(i)}$ is converted in time domain to reconstruct an estimated version of the OFDM block $\widehat{\mathbf{x}}^{(i)}$. Then, a detector is used to locate and replace the samples that are assumed to be clipped at the transmitter:

$$\forall n = 0\cdots N-1, \quad \widetilde{x}_n^{(i+1)} = \begin{cases} \widetilde{x}_n^{(0)} & \text{if } |\widehat{x}_n^{(i)}| \le A, \\ \widehat{x}_n^{(i)} & \text{if } |\widehat{x}_n^{(i)}| > A. \end{cases} \tag{7}$$

Hence, the time-domain output of the DAR loop is constituted of samples issued from the symbol decoder (those located at indices where clipping has been detected by the DAR loop) and of unaltered samples received from the channel

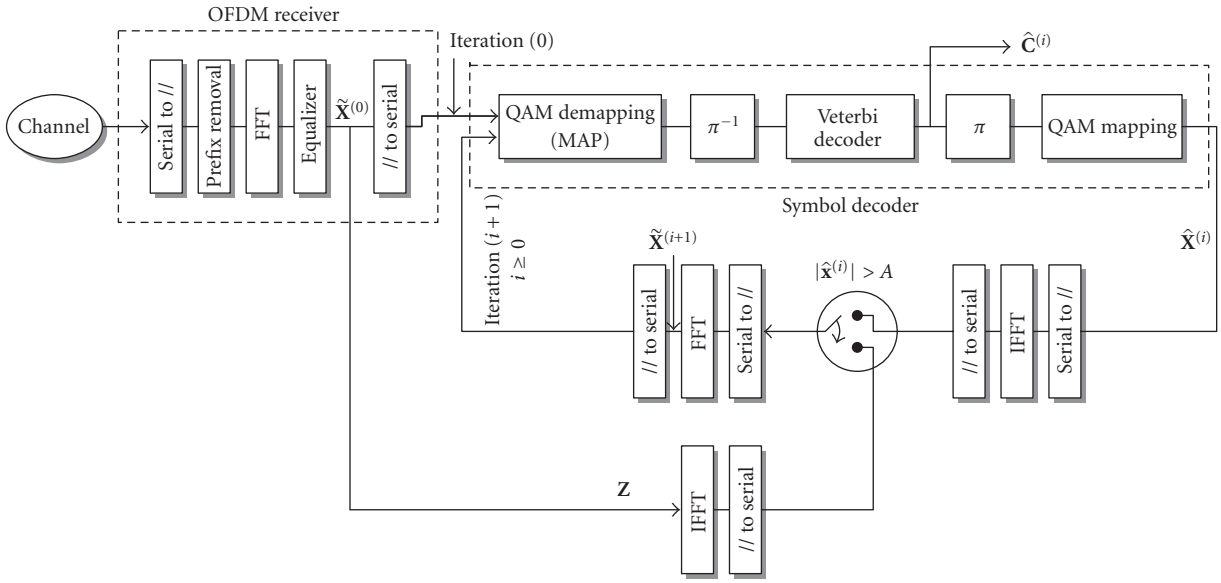

Figure 2: Principle of Turbo-DAR class of receivers.

(where no clipping is detected). These mixed samples are then used in the frequency domain as new noisy symbols for the input of the symbol decoder. Note that our system is strictly equivalent to a clipping noise n_{ck} estimation, followed by a subtraction step as follows:

$$n_{c_n}^{(i)} = \begin{cases} 0 & \text{if } \left|\widehat{x}_n^{(i)}\right| \leq A, \\ \widehat{x}_n^{(i)} - \widetilde{x}_n^{(0)} & \text{if } \left|\widehat{x}_n^{(i)}\right| > A, \end{cases} \qquad (8)$$
$$\widetilde{x}_n^{(i+1)} = \widetilde{x}_n^{(0)} - n_{c_n}^{(i)}.$$

We have chosen, in this work, to keep the DAR loop as reconstruction tool for the clipped samples, and our main concern is to try to increase the symbol protection in order to help the DAR loop at each iteration. Note that the DAR loop is not optimal because it does not take the clipping noise probability density function into account, and that other more efficient clipping noise mitigation methods can be proposed, based, for examble, on optimal Bayesian estimators [14], but at the expense of a large complexity increase. A receiver using the DAR reconstruction is a good tradeoff between implementation cost and performance.

As stated in [15], a 4-time oversampling is generally advised at the emitter before the clipping step for a efficient peak regrowth limitation. In that case, the DAR loop can easily be modified by using zero-padded IFFT as its input well as filtering and undersampling at its output.

The next subsection presents the structure of the simplest Turbo-DAR receiver. Then, two soft extensions of this algorithm are described and analysed in the next subsections.

3.2. The Hard-Turbo-DAR receiver

In this part, we briefly present the structure of the Hard-Turbo-DAR receiver. As in the original DAR method [10], the Hard-Turbo-DAR focusses on the design of a low-complexity receiver. As we assume convolutional coding in the OFDM system, the Viterbi algorithm is used as FEC decoder. Although using a hard decision decoder can appear to be inappropriate in a turbo loop, it has the advantage of a reduced receiver complexity compared to a *soft-input soft-output* (SISO) channel decoder. Such a receiver is clearly suboptimal, but the Hard-Turbo-DAR aims at correcting jointly the AWGN noise and the clipping noise with the minimum complexity.

The symbol decoder of the Hard-Turbo-DAR follows the three steps (see Figure 2) as follows.

(sd_1) from noisy symbols $\widetilde{\mathbf{X}}^{(i)}$, we build an interleaved *a posteriori* probabilities vector (denoted $\mathbf{app}_1^{\dagger(i)} = \{\mathrm{app}_1(C_{k,l}^{\dagger})^{(i)}\}_{k=0\cdots N-1,\, l=0\cdots \log_2(M)-1}$) at the bit level using a MAP QAM demapper:

$$\begin{aligned} \mathrm{app}_1\left(C_{k,l}^{\dagger}\right)^{(i)} &= P\left(C_{k,l}^{\dagger} \mid \widetilde{X}_k^{(i)}\right) \\ &= \sum_{s\in\mathcal{S}} P\left(C_{k,l}^{\dagger} \mid s\right) P\left(s \mid \widetilde{X}_k^{(i)}\right) \\ &\propto \sum_{s\in\mathcal{S}'} P\left(\widetilde{X}_k^{(i)} \mid s\right) \\ &\propto \sum_{s\in\mathcal{S}'} \exp - \frac{\left|\widetilde{X}_k^{(i)} - K_k H_k s\right|^2}{\left|K_k\right|^2 N_0}, \end{aligned} \qquad (9)$$

where $C_{k,l}^{\dagger}$ is the lth bit ($l = 0 \cdots \log_2 M - 1$) of the kth M-QAM symbol ($k = 0 \cdots N - 1$). The M-QAM constellation set is denoted $\mathcal{S}$ and $\mathcal{S}'$ is the subset of symbols with a binary mapping which has the lth bit equal to $C_{k,l}^{\dagger}$.

These APP are deinterleaved and used at the input of the Viterbi decoder. The input of the Viterbi decoder is then the APP vector $\mathbf{app}_1^{(i)} = \{\mathrm{app}_1(C_n)^{(i)}\}_{n=0..N_b-1}$ with the indices values $n = \pi^{-1}(k \log_2 M + l)$.

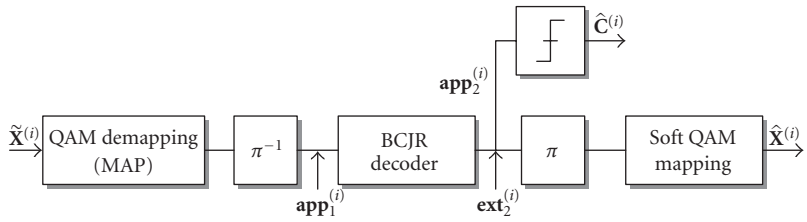

Figure 3: Structure of the Soft-Turbo-DAR symbol decoder.

(sd_2) the Viterbi decoder computes the maximum likelihood decoded sequence $\hat{\mathbf{C}}^{(i)}$. The decoded codeword is used to provide an estimation of the transmitted bits $\hat{\mathbf{U}}^{(i)}$ at the ith iteration, and also used to get estimated M-QAM symbols.

(sd_3) $\hat{\mathbf{C}}^{(i)}$ is interleaved, and hard mapped into symbols $\hat{\mathbf{X}}^{(i)}$ with $\hat{X}_k^{(i)} \in \mathcal{S}$. These estimated symbols are converted back to time domain using IFFT leading to $\hat{\mathbf{x}}^{(i)}$.

From the reconstruction and demapping (7) and (9), it can be noticed that the channel state information (CSI) is only valid at the first iteration; in the next iterations, the OFDM symbols $\widetilde{\mathbf{X}}^{(i)}, i > 0$ depend on the equalized OFDM symbols $\mathbf{Z}$ but also on the noiseless estimated OFDM frame $\hat{\mathbf{x}}^{(i)}, i > 0$. As a result, the noise power $|K_k|^2 N_0$ is generally misestimated for these iterations. Based on this remark, further improvement of the receiver could be possible. An example of CSI estimation algorithm followed by a scaling of the bits likelihoods at the input of the Viterbi decoder depending of the SNR in each subcarrier can be found in [16].

As pointed out in [12, 17], this algorithm behaves like a turbo receiver, despite the propagation of hard decided values. The "turbo effect" actually comes from the fact that the clipping noise is spread on all coded symbols in the frequency domain. So, the decoder which operates in the frequency domain takes benefits from this diversity. We will use this receiver for comparison with the improved receivers proposed in the next sections.

3.3. The Soft-Turbo-DAR receiver

The Hard-Turbo-DAR receiver clearly does not take full advantage from the turbo principle since the Viterbi decoder produces hard output values. In order to reach better performance, we propose in this section a more complex receiver based on an SISO channel decoder [18, 19]. In this paper, we only consider the BCJR decoder. The ouput of the decoder is composed of log-density-ratios which are reliability measures of the coded bits. In order to take advantage of these soft values, we propose to use a *soft symbol mapper* to produce soft symbols at the output of the symbol decoder. The soft symbols at the ith iteration are still denoted $\hat{\mathbf{X}}^{(i)}$, and can be interpreted as noisy M-QAM symbols. Because all values computed in the symbol decoder are soft, we called this receiver Soft-Turbo-DAR. As mentioned in the preceding section, the DAR loop is unchanged in all Turbo-DAR receivers, and only the symbol decoder is different. The three steps of the Soft-Turbo-DAR symbol decoder are as follows (cf. Figure 3).

(sd_1) This step is unchanged. The QAM demapper is still performed using the MAP criterion.

(sd_2) The deinterleaved APPs of the coded bits $\mathbf{app}_1^{(i)}$ (cf. (9)) are used at the input of the BCJR decoder to compute the extrinsic probabilities of the coded bits $\mathbf{ext}_2^{(i)} = \{\mathrm{ext}_2(C_n)^{(i)}\}_{n=0..N_b-1}$. These extrinsic values are obtained from the BCJR equations (cf. [18] for more details) using the following relation:

$$\forall n \in 0 \cdots N_b - 1, \quad \mathrm{ext}_2(C_n)^{(i)} \propto \frac{\mathrm{app}_2(C_n)^{(i)}}{\mathrm{app}_1(C_n)^{(i)}}, \tag{10}$$

where app_2 and ext_2 denotes respectively the *a posteriori* and the extrinsic output probabilities returned by the SISO decoder. The *a posteriori* probabilities are used to take a decision on the codeword $\hat{\mathbf{C}}^{(i)}$, or equivalently, the information bits $\hat{\mathbf{U}}^{(i)}$ at the last iteration.

(sd_3) The extrinsic probabilities are interleaved and propagated to the QAM mapper. At this stage, it is useful to take advantage of the soft values on the coded bits to build a soft QAM symbol based on the conditional mean estimator

$$\hat{X}_k^{(i)} = \sum_{C_{k,l}^{\dagger} \in \{0,1\},\ l=0\cdots\log_2 M-1} s \prod_{l=0}^{\log_2 M-1} \mathrm{ext}_2\left(C_{k,l}^{\dagger}\right)^{(i)}, \tag{11}$$

where s denotes the symbol labelled by the bits $\{C_{k,l}^{\dagger}\}_{l=0\cdots\log_2 M-1}$. The choice of the conditional mean estimator is discussed in conjonction with the binary mapping choice in Section 4. The output of the soft mapper is then a continuous value (in $\mathbb{C}$) that can be interpreted as a noisy M-QAM symbol, with the residual noise (additive noise plus clipping noise) present at the output of the FEC decoder at the ith iteration. The soft symbols $\hat{\mathbf{X}}^{(i)}$ are converted back to time domain using IFFT leading to $\hat{\mathbf{x}}^{(i)}$ that is used in the DAR loop. Note also that the soft symbols are obtained with the extrinsic probabilities, as in all turbo receivers.

3.4. An iterative BICM receiver using Turbo-DAR principle: Turbo-DAR-BICM

One further step can be reached in the direction of improving the symbol decoder by taking advantage of the inherent *bit*

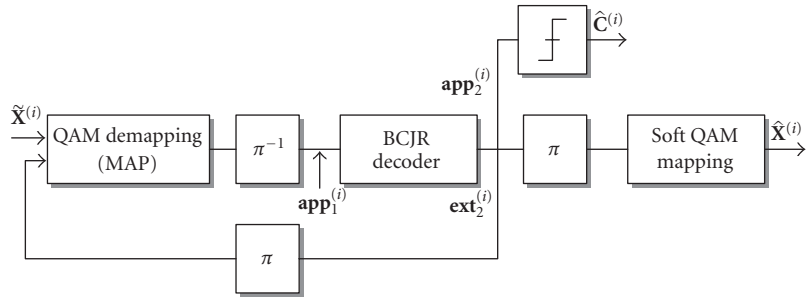

Figure 4: Structure of the Turbo-DAR-BICM symbol decoder.

interleaved coded modulation (BICM) structure of our transmission system (Figure 1). We propose in this section to feed back the extrinsic information at the SISO-FEC decoder to the input of the QAM demapper, as is done in iterative BICM receivers [20]. Consequently, the modified system now includes two loops. The overall complexity remains unchanged although the EXIT charts analysis (cf. Section 4) will show that this extra loop increases the number of iterations needed to achieve convergence.

We have seen that the Soft-Turbo-DAR receiver mitigates the clipping noise iteratively. However, it takes little advantage of all available soft information provided by the decoder for additive noise cancellation. As a matter of fact, it is possible to feed back the extrinsic probabilities $\mathbf{ext}_1^{(i)}$ to the input of the QAM demapper and use them as prior information for the next iteration. The structure of the symbol decoder is now depicted on Figure 4 and described thereafter.

(sd_2) This step is unchanged, the deinterleaved probabilities of the coded bits $\mathbf{app}_2^{(i)}$ are still used to compute the extrinsic LDR $\mathbf{ext}_1^{(i)}$ and the *a posteriori* probabilities $\mathbf{app}_1^{(i)}$ with the BCJR algorithm. Hence, the extrinsic probabilities are now used both to feed the soft mapper and the input of the QAM demapper at the next iteration.

(sd_3) The QAM soft mapper is also unchanged and the conditional mean estimator is still used. However, the question of the map-labelling choice is reopened since the binary labelling of the QAM constellation will now serve in the soft symbol mapper, but also in the BICM loop. The discussion of the map labelling will be illuminated in the next section with an EXIT chart study.

4. EXIT CHARTS ANALYSIS OF TURBO-DAR RECEIVERS

4.1. Analysis of the Soft-Turbo-DAR receiver

Although it increases significantly the overall complexity of the symbol decoder, the use of a soft-output BCJR decoder and a soft-symbol mapper allows the propagation of soft information during the decoding iterations leading to the so-called turbo principle. Additionaly to the performance improvement, this framework allows us to use the EXIT Charts proposed in [13] to analyse the behavior of the Soft-Turbo-DAR receiver. Indeed, the Soft-Turbo-DAR receiver can be considered as the concatenation of two *soft-Input soft-Output* modules. The first one (called DAR loop in the sequel) is constituted by the blocks which contain the soft mapper and demapper as well as the comparator with the clipping amplitude, FFT and IFFT components and the second one is the BCJR channel decoder.

At the ith iteration, the DAR-loop denoted $\mathcal{B}_1$ has input $\mathbf{ext}_2^{(i)}$ and output $\mathbf{app}_1^{(i+1)}$. Also at the ith iteration, the BCJR block denoted $\mathcal{B}_2$ has input $\mathbf{app}_1^{(i)}$ and extrinsic output $\mathbf{ext}_2^{(i)}$. Using these soft values, the extrinsic information content $I_{B_{1,2}}$ (in) and $I_{B_{1,2}}$ (out) expressed in bit-per-channel use (b/cu) are computed through Monte Carlo simulations under the Gaussian assumption according to the equations in [13, 21]. We can notice that the output of block $\mathcal{B}_1$ is not extrinsic to this block since it is not possible to remove the contribution of its input in a simple manner. This problem is mainly due to the soft symbol mapper and the FFT components. Despite this drawback, we show in this section that the EXIT chart analysis can fairly well predict the asymptotic behavior of Soft-Turbo-DAR receiver, and also that it helps us to choose the best binary mapping.

Choosing a good estimator of soft symbols from bit probabilities is not an easy problem, and is encountered in many other turbo receivers (turbo equalization [22] or turbo synchronization [23]). The main problem comes from the fact that the mapping of the QAM constellation (the bit labels of each symbol) is related to the properties of the soft symbol estimator. It is often adviced to rely on the Gray mapping combined to a conditional mean estimator to obtain good soft symbols [22, 23]. Using an EXIT charts analysis, we study the influence of the mapping choice on the Soft-Turbo-DAR receiver.

In Figure 5, we have drawn the EXIT chart at $E_b/N_0 = 8$ dB of block $\mathcal{B}_2$ corresponding to a convolutional code with generators $(5, 7)_{|8}$, and the EXIT chart of block $\mathcal{B}_1$ with two different types of binary mappings: the Gray mapping and the modified set-partitioning mapping (MSP mapping) [24].

For both mappings, the MI at the output of block $\mathcal{B}_1$ is constant when the input is lower than 0.5. This shows that in this area, the system does not take advantage from the iterative process. When the MI of $\mathcal{B}_1$ input is greater than 0.5, the output MI of the whole system progressively increases and the Soft-Turbo-DAR enters in its iterative

behavior. However, the convergence point lower than 1 prevents Gray- and MSP-mapping based systems from converging at $E_b/N_0 = 8$ dB to a very low bit error rate. The Gray mapping is clearly more advantageous for a Soft-Turbo DAR than the MSP mapping, so it appears that the Soft-Turbo-DAR algorithm is unable to use the information provided by high minimum squared Euclidean weight (MSEW) labelling as in BICM-ID receivers [25]. We will reconsider this conclusion in Section 4.

Finally, even for Gray labelling, the iterative process reaches a fixed point (where the 2 curves intersect) lower than 1 b/cu. So a residual error will remain asymptotical. However, the numerical result presented in Section 5 show that this residual error is low and that the Soft-Turbo-DAR receiver allows a significant performance improvement compared to the Hard-Turbo-DAR.

4.2. Discussion on the mapping choice for Turbo-DAR BICM based on EXIT charts

Because of its different structure, the conclusion on the mapping choice made for the Soft-Turbo DAR cannot be generalized to the Turbo-DAR BICM. In particular, we base our study on the fact that the choice of the labelling is a crucial issue in the design of BICM-ID receivers in order to achieve a high coding gain over the iterations. In [24, 25], it was shown that Gray labelling gives the best performance at the first decoding stage, but also achieves very low performance gain with further decoding iterations of the algorithm. In fact, the BICM-ID decoder takes advantage of a high MSEW of the constellation when correct extrinsic information issued from the decoder is used iteratively at the demapper input. Such high MSEW labellings were introduced in [24, 25]: among them, the modified set partitioning (MSP), which exhibits a free Euclidean distance which is twice that of the Gray mapping, is presented as a good labelling map for QAM signaling on both fading and AWGN channels.

The mapping choice cannot be directly generalized from the BICM-ID to the Turbo-DAR BICM, due to the presence of the soft mapping block in our receiver. The soft mapping block builds soft symbols from the *binary* extrinsic probabilities, using a conditional mean estimator. The MSP mapping is not a good choice for the soft mapping block because symbols with high reliability are spread everywhere in the constellation, contrary to the Gray mapping case, where symbols with high reliability are more concentrated. As a consequence, the output of the soft mapper with MSP mapping is biased and concentrated around the origin of the QAM constellation. Therefore, the choice of the mapping has to be balanced between the behavior of the soft mapper and that of the BICM-ID decoder. A solution based on the use of the MIX mapping introduced in [24], which provides a mixed design between MSP and Gray mapping, is proposed in this paper, and we show by EXIT charts analysis that it provides a good tradeoff between the BICM-ID structure and an enhanced DAR-loop behavior.

Figure 6 draws the EXIT charts of the Turbo-DAR-BICM receiver for differently labeled 16-QAM constellations. The previous discussion is confirmed by the EXIT charts. The tunnel is more open with the MIX mapping compared to the MSP mapping. Note that the tunnel for the MSP mapping is open at the considered $(E_b/N_0)_{\text{dB}}$. The drawback of the MIX mapping is that it seems that the Turbo-DAR BICM converges to a fixed point which is not equal to 1 b/cu. This means that we expect a residual error floor when using the MIX mapping in the Turbo-DAR BICM. However, the fixed point is very close to 1 b/cu, so the error floor can be very low in practice, and this problem can be efficiently solved

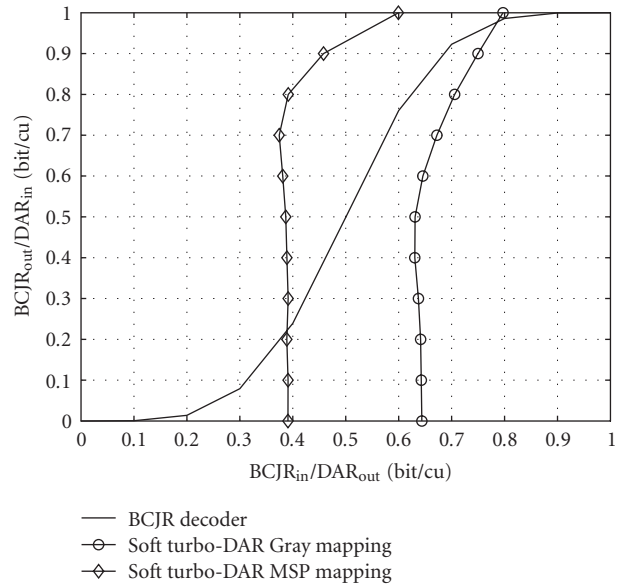

Figure 5: EXIT charts of the Soft-Turbo-DAR receiver over AWGN channel with CR = 1dB, $N = 64$, $E_b/N_0 = 8$ dB. The curve in solid line with circles corresponds to the EXIT function of the DAR loop with *Gray mapping* and that in solid line with diamonds represents the EXIT function with *MSP mapping*.

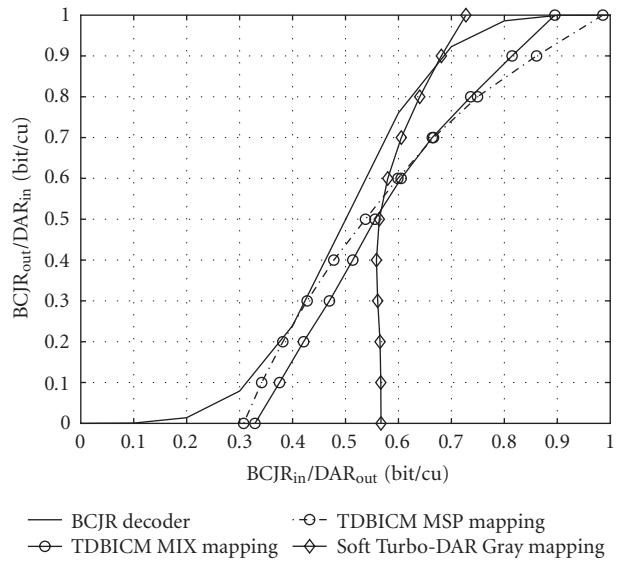

Figure 6: EXIT charts of Soft-Turbo-DAR and Turbo-DAR-BICM at $E_b/N_0 = 5.5$ dB and CR = 1 dB (AWGN channel).

by using an extra outer error-correcting code with very high rate. Also, it can be noticed that the Turbo-DAR BICM performs better that the Soft Turbo-DAR with Gray mapping after convergence. Although not presented, the EXIT chart of Turbo-DAR BICM with Gray mapping is similar to the Soft-Turbo DAR with Gray mapping: it was expected since a Gray mapping does not bring any performance improvement in a BICM-ID-based receiver.

As a conclusion, the use of MIX labelling provides a compromise between the DAR loop and the symbol decoder, and we will verify this statement with finite length simulations in the next section.

5. PERFORMANCE COMPARISON

5.1. Comparison between Hard-Turbo-DAR and Soft-Turbo-DAR receivers

In this section, we present simulation results of the Soft-Turbo DAR, and compare it to the Hard-Turbo DAR and other types of receivers. The system parameters are $N = 64$ 16-QAM symbols per OFDM block with Gray mapping, and a very severe clipping ratio of CR = 1 dB. In Figure 7, we present the simulations over an AWGN channel, and Figure 8 presents the results over a STVFS channel. The considered STVFS channel is composed of a 12-tap delay line dispersive channel with independent random complex coefficients distributed as $\mathcal{N}(0, \exp(-\beta n))$ where $n = 0 \cdots 11$ and β is fixed to 2.5 for our simulations. This value of β has been chosen to exhibit frequency fades up to -20 dB. Also, new channel realizations are considered for each OFDM block in order to model a block-stationarity behavior.

In each case, we compared four different receivers to a lower bound (corresponding to a system without clipping and a BCJR as channel decoder). The four receivers are as follows.

(1) FEC-only: a receiver with no clipping noise mitigation, which means that only the BCJR decoder tries to correct the Gaussian noise *and* the clipping noise,
(2) DAR + FEC: a receiver which uses a DAR clipping noise mitigation before the BCJR decoder. Several iterations of a DAR loop are used to mitigate the clipping noise, then log-likelihood ratios are computed from the corrected channel observations, and used as initialization for the BCJR decoder.
(3) Hard-Turbo DAR: the iterative receiver described in Section 3.2. Only four iterations are used because the convergence of this iterative receiver is very fast due to the hard decisions taken in the loop.
(4) Soft-Turbo DAR: the improved receiver described in Section 3.3. Only four iterations of this receiver were also used since more iterations showed only minor improvements.

Figures 7 and 8 clearly illustrate the effectiveness of the Turbo-DAR receivers when the clipping noise is strong. For the AWGN channel, at such a low clipping ratio, the DAR + FEC receiver provides very little BER improvement whereas at BER $= 10^{-4}$, the Hard-Turbo-DAR receiver performs more than 3 dB better than existing receivers, and another 2 dB gain is obtained with the Soft-Turbo DAR. We can see in Figure 8 that similar comments can be made for the STVFS channel, which shows the robuteness of our approach to the transmission channel spectrum.

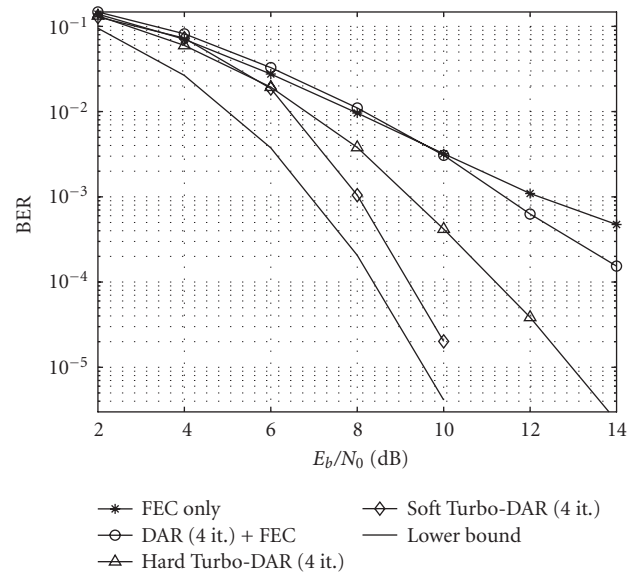

Figure 7: BER performance comparison of different receivers in the presence of clipping noise over AWGN channel. Only the last iteration of the receivers is shown. The parameters are CR = 1 dB, $N = 64$, and a 16-QAM with Gray mapping.

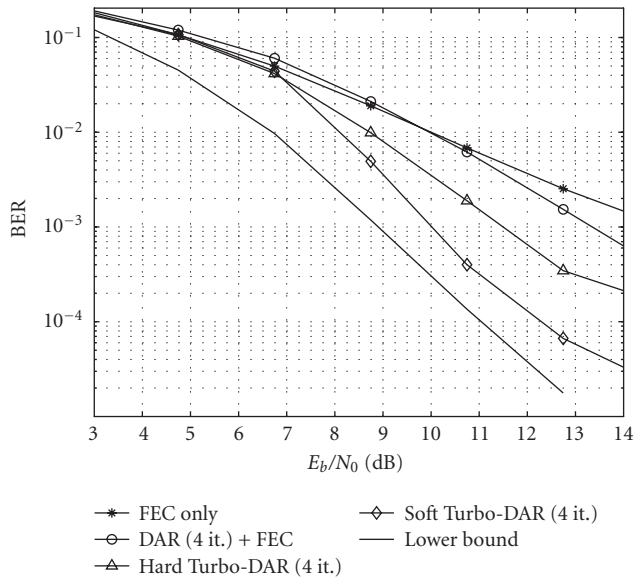

Figure 8: BER performance comparison of different receivers in the presence of clipping noise over STVFS channel. Only the last iteration of the receivers is shown. The parameters are CR = 1 dB, $N = 64$, and a 16-QAM with Gray mapping.

Those results show that the complexity increase of the Soft-Turbo-DAR receiver is justified by the performance gain that is observed. Also, the Soft-Turbo DAR operates quite

close to the lower bound ($\simeq$1 dB), which shows that this receiver is close to optimal despite the use of suboptimal components like the soft symbol mapper and the DAR loop.

As a conclusion, we stress the fact that the Turbo-DAR receivers are very interesting solutions since they can compensate for a great part of clipping noise even at very severe clipping ratios. The CR is fixed here at 1 dB while it is usually fixed around 4-5 dB in existing OFDM systems.

5.2. Performance improvement brought by the Turbo-DAR-BICM receiver

The asymptotical results given by the EXIT charts for the AWGN channel are confirmed by the BER performance presented in Figure 9. In this figure, we compare the Turbo-DAR-BICM receiver with MIX and MSP mappings with the results of the Soft-Turbo DAR, and with the corresponding lower bounds, that is, a BICM-ID receiver without any clipping noise.

As expected, the Turbo-DAR BICM with the MIX mapping performs better than with the MSP mapping in the convergence region as a performance gain of more than 1 dB is seen up to a BER $= 10^{-4}$. The error floor predicted by the EXIT charts analysis appears at BER $= 10^{-5}$. The performance gain compared to the Soft-Turbo DAR is very important, and shows the interest of feeding back the soft extrinsic values to the demapper, with a relatively small complexity increase. Also, the Turbo-DAR-BICM curves are not too far from the lower bounds, but there is still some gap to be filled and this opens prospects for further research.

Again, we show that our receivers are robust to the frequency selectivity of the channel by plotting results for a STVFS channel in Figure 10, although, the gap to the lower bounds is much larger in this case.

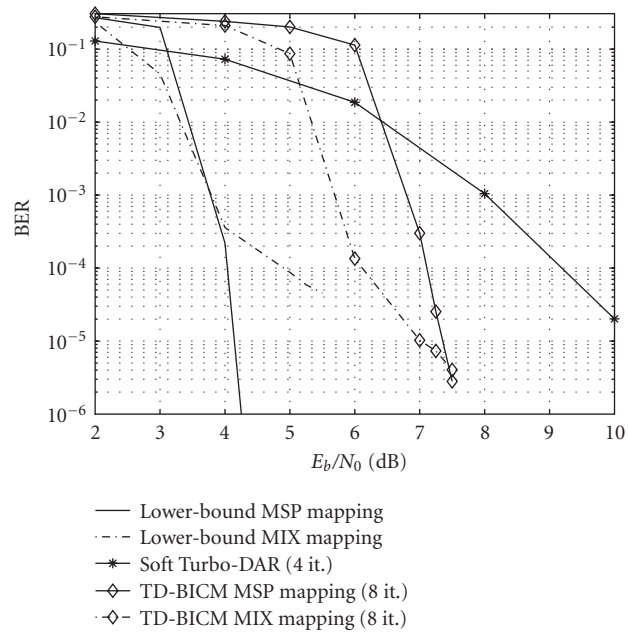

Figure 9: BER comparison of the Turbo-DAR-BICM (MIX and MSP mappings) with the Soft-Turbo-DAR for AWGN channel with 16-QAM, CR = 1 dB, $N = 64$.

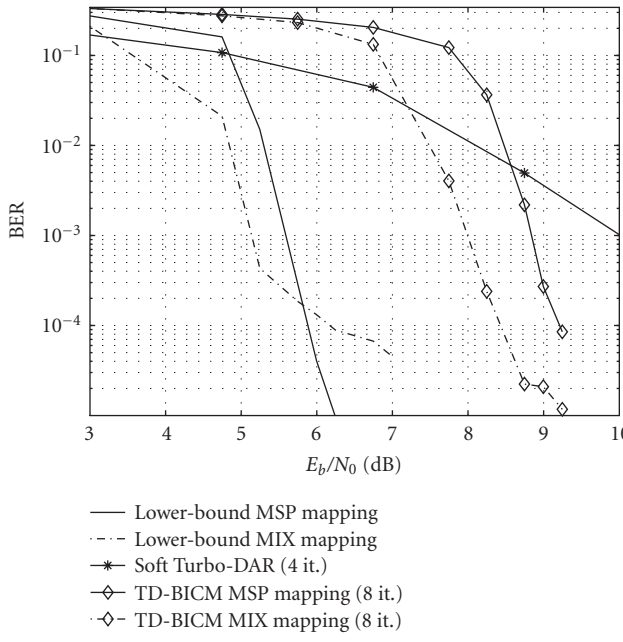

Figure 10: BER comparison of the Turbo-DAR-BICM (MIX and MSP mappings) with the Soft-Turbo-DAR for the STVFS channel, the parameters of the receiver are the same as those in Figure 8.

6. CONCLUSION

In this paper, we have proposed three receivers with growing complexity and performance for clipping noise mitigation.

The Turbo-DAR receivers combine iteratively the clipping level information and the FEC decoder in order to provide an overall correction that greatly outperforms the "DAR + FEC" receiver.

The introduction of an FEC inside the DAR loop enables the mitigation of the clipping noise with CR as low as 1 dB. Such a strong clipping level allows to consider IBO at the transmitter such that no further saturation occurs even after *digital to analog* conversion. The introduction of a MAP decoder and a soft symbol mapper in the DAR loop enable the exchange of soft information between the decoder and the clipping noise reconstruction. This modification improves the performance results of more than 2 dB at BER $= 10^{-4}$ with respect to the Hard-Turbo DAR for both AWGN and STVFS channels, but at the expense of an extra computational complexity. An EXIT chart analysis shows that the Gray mapping is the best suited for the Soft-Turbo-DAR algorithm: it means that this receiver can be applied to many existing multicarrier standards (e.g., IEEE 802.11a or Hiperlan II) without any transmitter modification.

As our iterative receiver partially relies on a BICM scheme, the Soft-Turbo-DAR receiver can easily be modified to jointly behave as a DAR system and a BICM-ID decoder. With this modification, even the nonclipped samples are processed at each iteration. The Turbo-DAR-BICM receiver strongly depends on the map labelling choice and the

EXIT charts analysis shows that a mixed mapping provides a good tradeoff between the labelling needed by the *a posteriori* soft symbol mapper and high MSEW needed by the BICM-ID decoder.

The proposed receivers are still away from the lower bounds, which seems to indicate that some improvement can still be done. As a matter of fact, we did not question in our work the DAR block, and one can wonder if the replacement of the clipped samples only in the DAR loop is still efficient when a capacity-approaching coding scheme is used. In that case, performance improvement is expected by the investigation of other (and probably more complex) clipping noise estimators in the feedback loop. Future work will focus on this last point.

REFERENCES

[1] A. R. S. Bahai and B. R. Saltzberg, *Multi-Carrier Digital Communications: Theory and Applications of OFDM*, Kluwer Academic/Plenum Publishers, New York, NY, USA, 1999.

[2] L. Hanzo, M. Münster, B. J. Choi, and T. Keller, *OFDM and MC-CDMA for Broadband Multi-User Communications, WLANs and Broadcasting*, John Wiley & Sons, New York, NY, USA, 2003.

[3] T. M. Nguyen, J. Yoh, C. H. Lee, H. T. Tran, and D. M. Johnson, "Modeling of HPA and HPA linearization through a predistorter: global broadcasting service applications," *IEEE Transactions on Broadcasting*, vol. 49, no. 2, pp. 132–141, 2003.

[4] A. N. D'Andrea, V. Lottici, and R. Reggiannini, "Nonlinear predistortion of OFDM signals over frequency-selective fading channels," *IEEE Transactions on Communications*, vol. 49, no. 5, pp. 837–843, 2001.

[5] R. W. Bäuml, R. F. H. Fischer, and J. B. Huber, "Reducing the peak-to-average power ratio of multicarrier modulation by selected mapping," *Electronics Letters*, vol. 32, no. 22, pp. 2056–2057, 1996.

[6] H. Breiling, S. H. Müller-Weinfurtner, and J. B. Huber, "SLM peak-power reduction without explicit side information," *IEEE Communications Letters*, vol. 5, no. 6, pp. 239–241, 2001.

[7] L. J. Cimini Jr. and N. R. Sollenberger, "Peak-to-average power ratio reduction of an OFDM signal using partial transmit sequences," *IEEE Communications Letters*, vol. 4, no. 3, pp. 86–88, 2000.

[8] H. Ochiai and H. Imai, "Performance analysis of deliberately clipped OFDM signals," *IEEE Transactions on Communications*, vol. 50, no. 1, pp. 89–101, 2002.

[9] X. Li and L. J. Cimini Jr., "Effects of clipping and filtering on the performance of OFDM," *IEEE Communications Letters*, vol. 2, no. 5, pp. 131–133, 1998.

[10] D. Kim and G. L. Stüber, "Clipping noise mitigation for OFDM by decision-aided reconstruction," *IEEE Communications Letters*, vol. 3, no. 1, pp. 4–6, 1999.

[11] J. Tellado, L. M. C. Hoo, and J. M. Cioffi, "Maximum-likelihood detection of nonlinearly distorted multicarrier symbols by iterative decoding," *IEEE Transactions on Communications*, vol. 51, no. 2, pp. 218–228, 2003.

[12] H. Chen and A. M. Haimovich, "Iterative estimation and cancellation of clipping noise for OFDM signals," *IEEE Communications Letters*, vol. 7, no. 7, pp. 305–307, 2003.

[13] S. ten Brink, "Convergence behavior of iteratively decoded parallel concatenated codes," *IEEE Transactions on Communications*, vol. 49, no. 10, pp. 1727–1737, 2001.

[14] D. Declercq and G. B. Giannakis, "Recovering clipped OFDM symbols with Bayesian inference," in *Proceedings of the IEEE International Conference on Acoustics, Speech, and Signal Processing (ICASSP '00)*, vol. 1, pp. 157–160, Istanbul, Turkey, June 2000.

[15] J. Tellado, *Peak to average power reduction for multicarrier modulation*, Ph.D. thesis, Standford University, Stanford, Calif, USA, 1999.

[16] Y. Wang, J. H. Ge, B. Ai, P. Liu, and S. Y. Yang, "A soft decision decoding scheme for wireless COFDM with application to DVB-T," *IEEE Transactions on Consumer Electronics*, vol. 50, no. 1, pp. 84–88, 2004.

[17] G. Gelle, M. Colas, and D. Declercq, "Turbo decision aided reconstruction of clipping noise in coded OFDM," in *Proceedings of the 5th IEEE Workshop on Signal Processing Advances in Wireless Communications (SPAWC '04)*, pp. 591–595, Lisbon, Portugal, July 2004.

[18] L. Bahl, J. Cocke, F. Jelinek, and J. Raviv, "Optimal decoding of linear codes for minimizing symbol error rate," *IEEE Transactions on Information Theory*, vol. 20, no. 2, pp. 284–287, 1974.

[19] J. Hagenauer and P. Hoeher, "A viterbi algorithm with soft-decision outputs and its applications," in *Proceedings of the IEEE Global Telecommunications Conference (GLOBECOM '89)*, vol. 3, pp. 1680–1686, Dallas, Tex, USA, November 1989.

[20] X. Li and J. A. Ritcey, "Bit-interleaved coded modulation with iterative decoding," *IEEE Communications Letters*, vol. 1, no. 6, pp. 169–171, 1997.

[21] T. J. Richardson and R. L. Urbanke, "The capacity of low-density parity-check codes under message-passing decoding," *IEEE Transactions on Information Theory*, vol. 47, no. 2, pp. 599–618, 2001.

[22] D. Leroux, C. Laot, and R. Le Bidan, "Low-complexity MMSE turbo equalization: a possible solution for EDGE," *IEEE Transactions on Wireless Communications*, vol. 4, no. 3, pp. 965–974, 2005.

[23] C. Herzet, V. Ramon, L. Vandendorpe, and M. Moeneclaey, "EM algorithm-based timing synchronization in turbo receivers," in *Proceedings of the IEEE International Conference on Acoustics, Speech, and Signal Processing (ICASSP '03)*, vol. 4, pp. 612–615, Hong Kong, April 2003.

[24] A. Chindapol and J. A. Ritcey, "Design, analysis, and performance evaluation for BICM-ID with square QAM constellations in Rayleigh fading channels," *IEEE Journal on Selected Areas in Communications*, vol. 19, no. 5, pp. 944–957, 2001.

[25] F. Schreckenbach, N. Görtz, J. Hagenauer, and G. Bauch, "Optimization of symbol mappings for bit-interleaved coded modulation with iterative decoding," *IEEE Communications Letters*, vol. 7, no. 12, pp. 593–595, 2003.